Supporting Information

Electrooxidation of Pd-Cu NPs loaded porous carbon derived from Cu-MOF

Salma Mirza,[ab] *Hao Chen,* [a] *Zhi-Gang Gu**[a] *and Jian Zhang*[a]

[a] State Key Laboratory of Structural Chemistry, Fujian Institute of Research on the Structure of Matter, Chinese Academy of Sciences, Fuzhou, Fujian 350002, P.R. China.

[b] University of Chinese Academy of Sciences, Beijing, 100049, P.R. China.

Corresponding E-mail: zggu@fjirsm.ac.cn

Experimental Section

Materials and instrumentation

All reagents were commercially available and used without any purification. Nafion® Dispersion solution DE 520 CS type (Wako Pure Chemical Industries, Ltd.) and Pd/C (Carbon, Cabot Corp., USA) were used as received. The Powder X-ray diffractometer (PXRD, MiniFlex2 X-ray diffractometer) was used to recognize the phases contain in the prepared powder sample with CuKα radiation (λ = 0.1542nm). Scanning Electron Microscopy (SEM: JSM6700), Transmission Electron Microscopy (TEM) with EDS mapping, TEM energy dispersion spectroscopy (TEM-EDS, JEM-2010F instrument). Scanning electron microscope (SEM) images were measured by JSM6700. Electrochemical measurement was carried out by Zahner-Zennium IM6. Inductive Couple Plasma (ICP, Ultima 2 instrument) and X-Ray Photoemission Spectroscopy (XPS) analysis (ESCALAB 250Xi) has been carried out to examine, elemental composition and their micro level structural morphology studied.

Synthesis of HKUST-1

Hydrothermal synthesis protocol has been used for the HKUST-1 preparation.[1] BTC was taken 2 mmol (0.42 g) to dissolve in a mixture of ethanol and deionized water in 50:50 vol. %. This mixture was put for stirring around 10 min to obtain a clear solution. Afterward 3.62 mmol (0.875 g) of $Cu(NO_3)_2.3H_2O$ was put in the solution while stirring thoroughly for a further 10 min. after the reactants fully dissolved Once the reactants were completely dissolved in the solvent, the blue solution obtained and then shifted to Teflon lined stainless steel autoclave and subjected to heat on 100 ^oC for 24 h. Then the blue crystalline powder as obtain was subjected to filtration and thoroughly washing with a mixture of 50 % v/v water and ethanol. The crystalline powder put in the oven at 60 ^oC to precede new experiments.

Preparation of HKUST-1 derived carbon (Cu/C)

The 2.0 g of HKUST-1 was taken into a ceramic boat and then put it into a temperature-automatic furnace under nitrogen flow for 1.5 hrs. Consequently, the sample was prepared heating to 700 °C and temperature was kept to 5 hrs. Under continuous nitrogen flow the sample was cooled down to room temperature. The black carbonized materials were taken out from the furnace and then washed with deionized water and dried at 80 °C for 1 h to obtain the HKUST-1 derived carbon porous material (symbolized as Cu/C). The yield of the product was achieved about 22 %.

Preparation of Pd-Cu/C NPs

Ethanolic solution of $PdCl_2$ (super saturated, 10 mL) was added into a obtained Cu/C and dried for 30 min at 80 ^oC temperature, and then calcinated again in an automatic furnace at 300 ^oC for 1 h in order to obtain the Pd-Cu/C catalyst.

Electrochemical characterizations

Figure S1 shows cyclic voltammogram of Pd-Cu/C and commercial Pd/C in 1.0 mol L^{-1} KOH solution. The anodic peaks were clearly seen in the voltammogram which indicated the electrochemical reaction occurred on the surface of the electrode. Peak A1 and A1' appeared at -0.79 V for Pd/C while at -0.40 V for Pd-Cu/C electrocatalysts respectively in eq. (1). The shift in hydrogen absorption/desorption region at higher potential in Pd-Cu/C was mainly because of Cu in our material.[2,3,4] The -OH adsorption peaks A2 (-0.11 V) and A2' (-0.15 V) for Pd/C and Pd-Cu/C observed because of formation of Pd-OH in eq.(2) while A2' occurs with the onset potential of Palladium oxidation and overlaps with the hydrogen desorption peak as shown in eqs.(3) and (4).[5,6] Moreover, the beginning of Pd-OH formation for Pd-Cu/C were more negative than Pd/C. This means that Cu_2O and CuO effect the Pd-OH formation. This lead to the transmetallation reaction and forming Cu-OH at more positive potential in Pd-Cu/C as follows eq (6). The Cu (0) or Cu (I) oxidation peaks was not observed for Pd-Cu/C while peak potential A3' (E^0 = -0.08 V) for Cu (I)/Cu(II) electronic transitions in eqs. (5). Subsequently the formation of Pd-O overlaps with the Pd-OH for Pd-Cu/C with peak potential -0.18 V as peak A4' and A3 at around -0.41 V for Pd/C shown in eq. (7).[7,8] Two cathodic peaks appeared at C1 (-0.48 V) and C1' (-0.35 V) with respective Pd/C and Pd-Cu/C characterized by the PdO reduction to Pd-OH (eq. 7). However, peaks C2 (-0.42 V) and C2' (-0.45V) for Pd/C and Pd-Cu/C can be attributed for reduction of Pd-OH to Pd in eq. 6.[9] The negative shift in the reduction potential of Pd-OH for Pd-Cu/C than that of Pd/C demonstrated the alloying of Cu with the Pd in our electrocatalyst affects the potential and Pd-OH is comparatively less stable in Pd-Cu/C electrode than Pd/C. The ratio of peak current densities IA2' /IA2 (5.32/0.45 = 12) for Pd-OH formation was very high. The current density for the Pd-OH formation was ~12 times higher than the commercial Pd/C, suggesting that copper oxides existence is kinetically favored hydroxylation and about ~12 times higher ability of Pd-OH formation by our synthesized Pd-Cu/C NPs.[10,11]

Electrode preparation and electrochemical performance test

5 mg of Pd-Cu/C; 0.5 mL of ethanol and 20 μL of Nafion solution were allowed to mix in ultrasonicator for about 2 hs. After that uniformly mixed 3 μL of the catalyst ink was deposit on the GC-RDE surface *via* a micropipette syringe and let it dry for about 10 minutes at room temperature.

Electrochemical surface area calculation:

The ECASA is an important factor in electrochemical measurements. The performance of Pd-Cu/C electrocatalyst was evaluated by electrochemical active surface area (ECASA) of electrode, which was often calculated using charge associated with the reduction of PdO by integrating the area under cathode peak ($Q = mC\ cm^{-2}$) during the CVs at scan rate 50 mVs^{-1} for Pd-Cu/C and commercial Pd/C are 258 and 11 respectively in Figure S1. The ECASA of Pd-Cu/C in Figure S1. The reduction of PdO monolayer 405 μC cm^{-2} was required.[12] The ECASA was determined by using the equation.

ECASA = Q / (0.405 / [Pd]).[13]

Charge (Q) = Area / Scan rate

Where the ECSA was calculated in m^2g^{-1}, Q represents charge in mC cm^{-2} and [Pd] represents loading of Pd (mg cm^{-2}) in electrode.

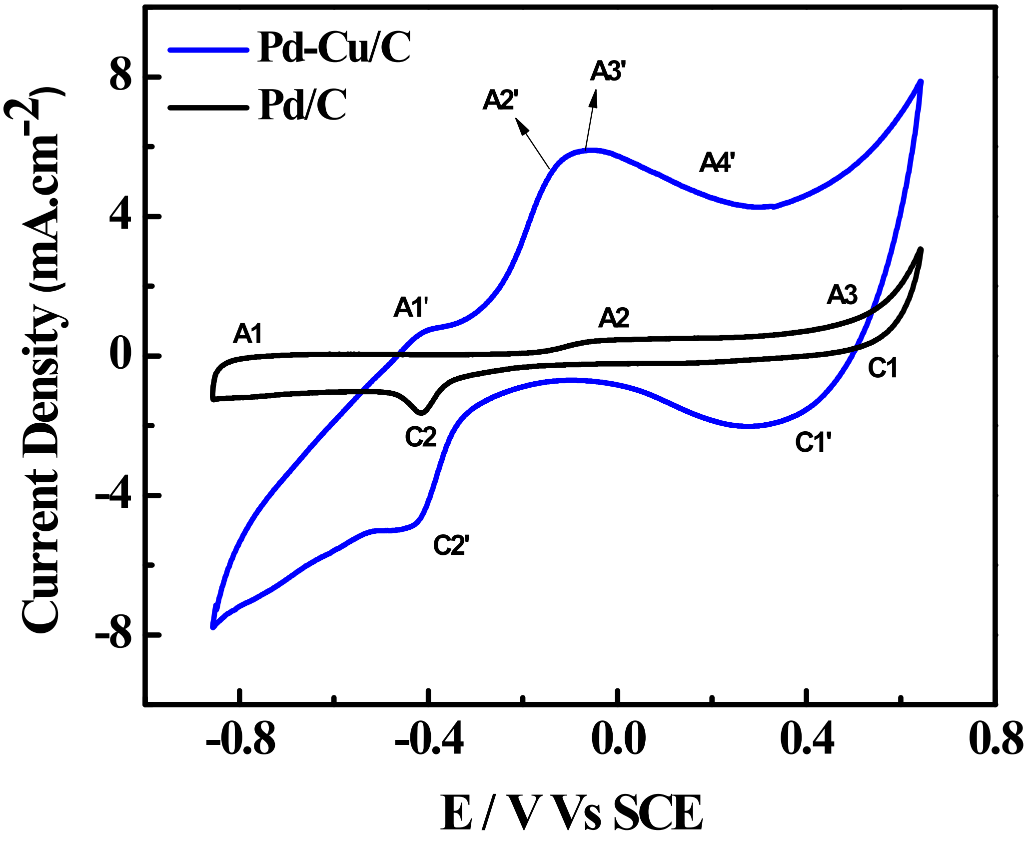

Figure S1. CV curves of Pd/C and Pd-Cu/C electrocatalyst in 1 M KOH solution at a scan rate of 50 mV s^{-1} at room temperature.

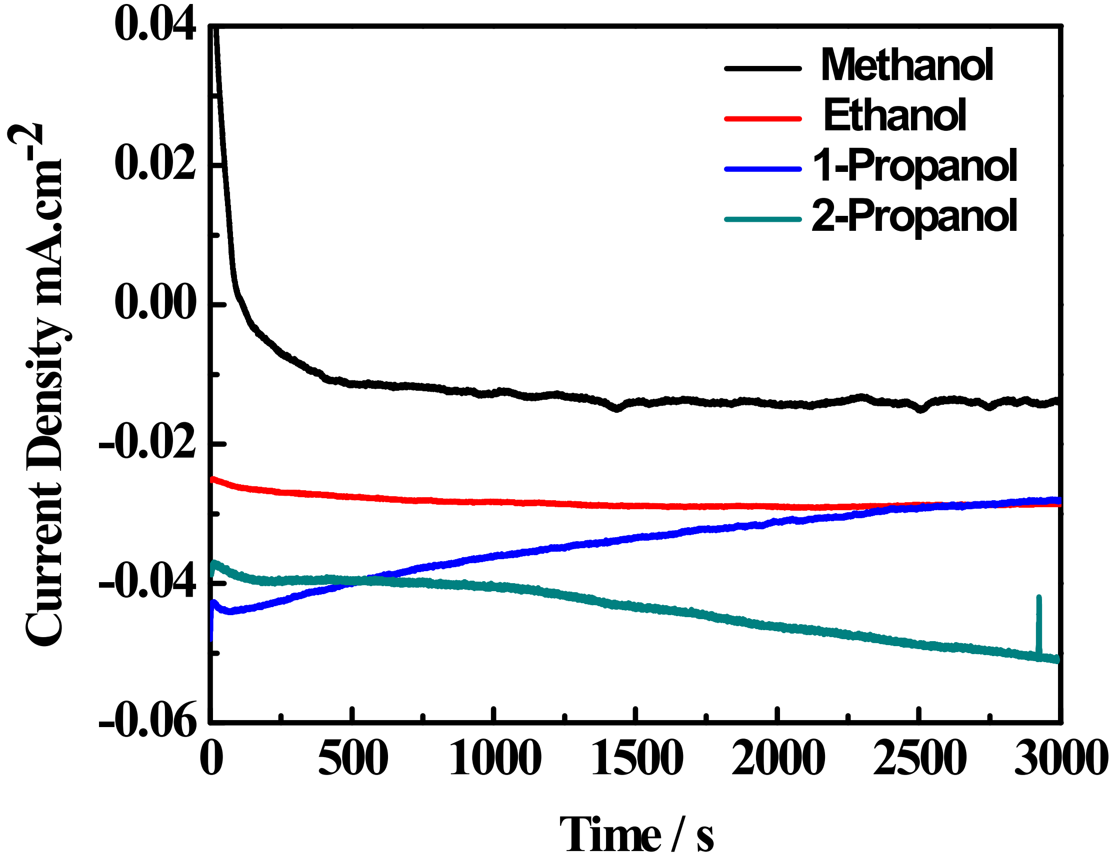

Figure S2. Chronoamperometric measurements of Pd-Cu/C electro catalyst in 1M C_1-C_3 alcohol solution containing 1 M KOH at – 0.25V

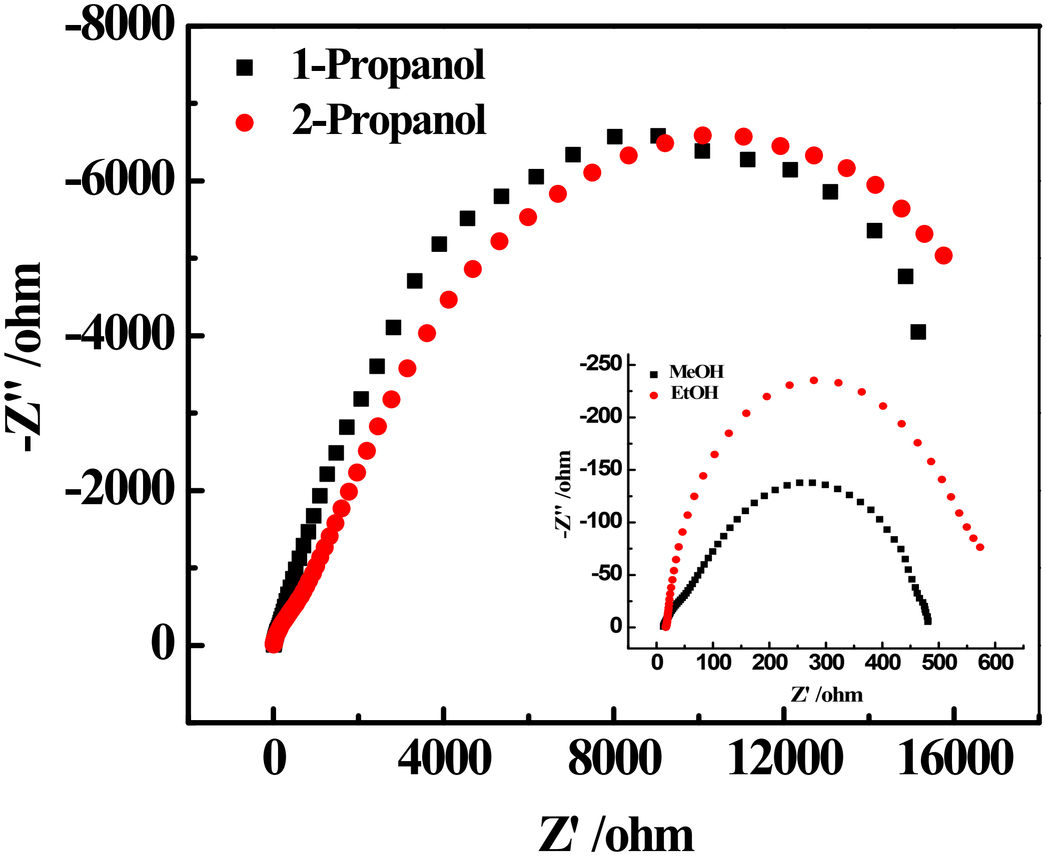

Figure S3. The Nyquist plot of Pd-Cu/C electro catalyst in 1M KOH containing 1 M C_1-C_3 alcohols at -0.4 V.

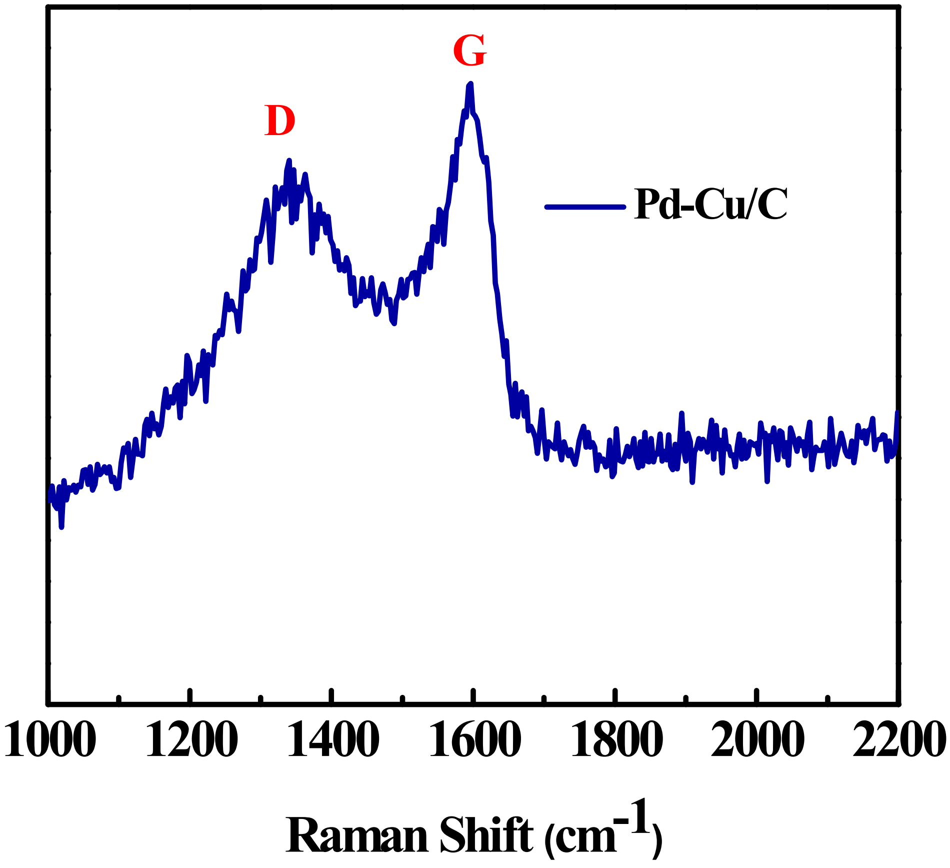

Figure S4. The Raman spectrum of Pd-Cu/C material, typical graphitic bands identified as G: peak for graphite at 1332 cm^{-1}; D: peak that means disorder at 1596 cm^{-1}.

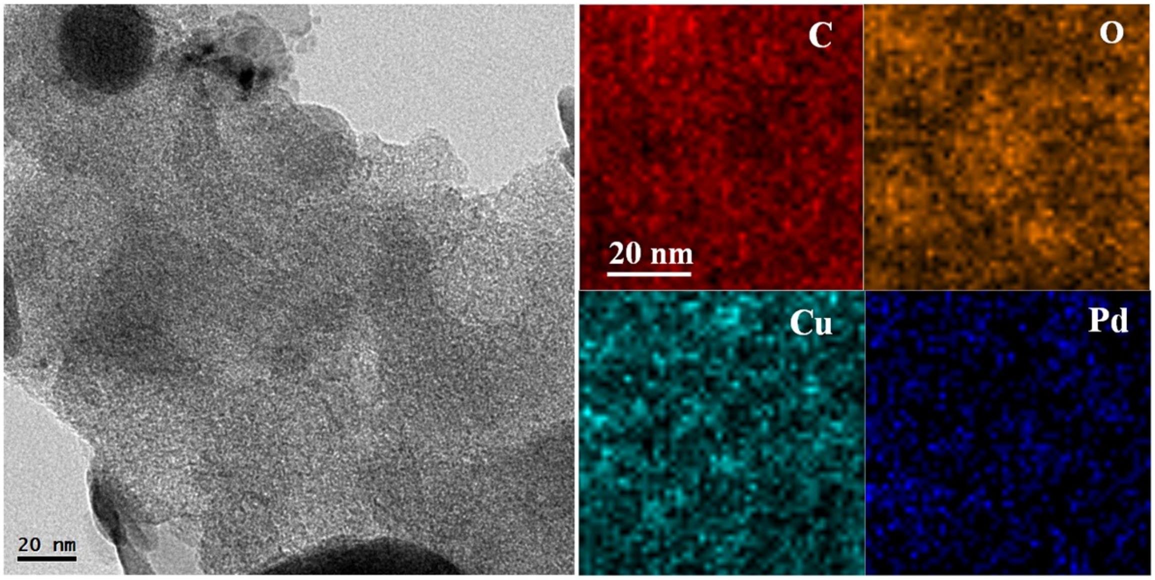

Figure S5. TEM mapping (C, O, Cu and Pd) of Pd-Cu/C NPs.

Table S1. Elemental composition of Pd-Cu/C *via* ICP and CHN analysis

Sample	**ICP %**		**CHN**		
	Pd	Cu	C	H	N
Pd-Cu/C	4.63	36.68	21.14	1.03	<0.3

Table S2. Electrochemical Performance of Pd/C and Pd-Cu/C electrodes for the oxidation of alcohols (C_1-C_3) in KOH (1M) solution.

Catalyst	**Onset Potential E_{on} (V)**	**Anodic Peak Potential EF (V *vs* SCE)**	**Anodic Peak Current iF (mA mg^{-1})**	**Backward Peak Potential EB (V *vs* SCE)**	**Backward Peak Current iB (mA mg^{-1})**	**iF/iB**
Methanol						
Pd/C	-0.42	-0.01	354	-0.39	52	6.80
Pd-Cu/C	-0.45	-0.16	4643	-0.37	205	22.64
Ethanol						
Pd/C	-0.60	-0.19	872	-0.38	506	1.7
Pd-Cu/C	-0.62	-0.22	139	-0.38	74	1.9
1-Propanol						
Pd/C	-0.60	-0.17	923	-0.38	652	1.4
Pd-Cu/C	-0.59	-0.21	94	-0.37	54	1.7
2-Propanol						
Pd/C	-0.65	-0.3	180	-0.46	11	16
Pd-Cu/C	-0.57	-0.27	26.5	-0.39	4.9	5.4

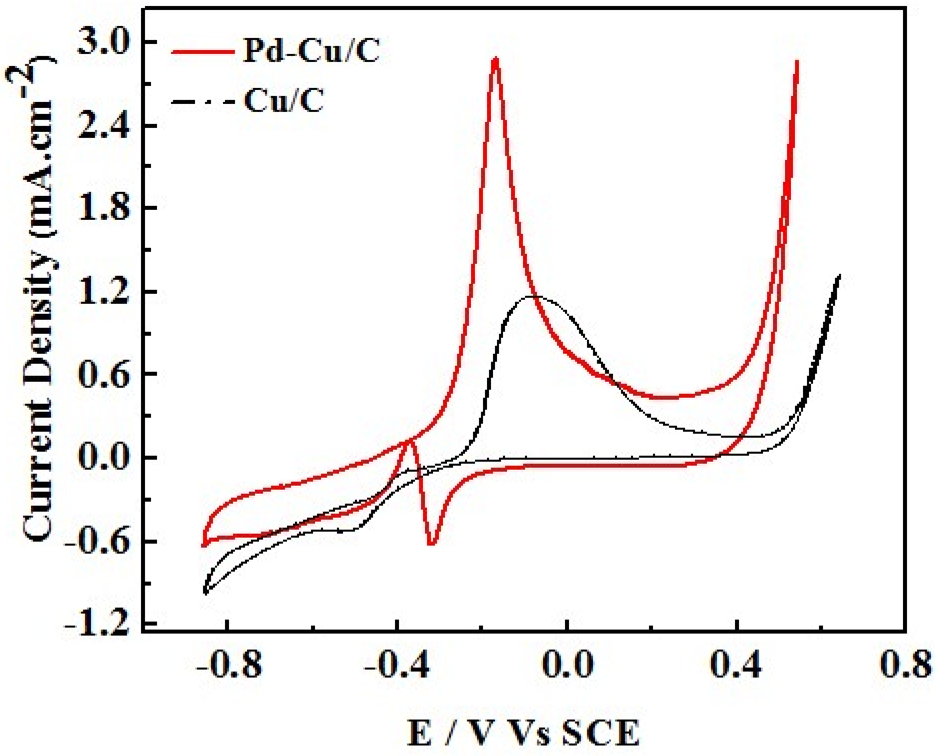

Figure S6. Cyclic voltammetric studies of Pd-Cu/C and Cu/C catalyst for oxidation in 1M MeOH containing 1 M KOH solution at a scan rate of 50 mV s^{-1} at room temperature.

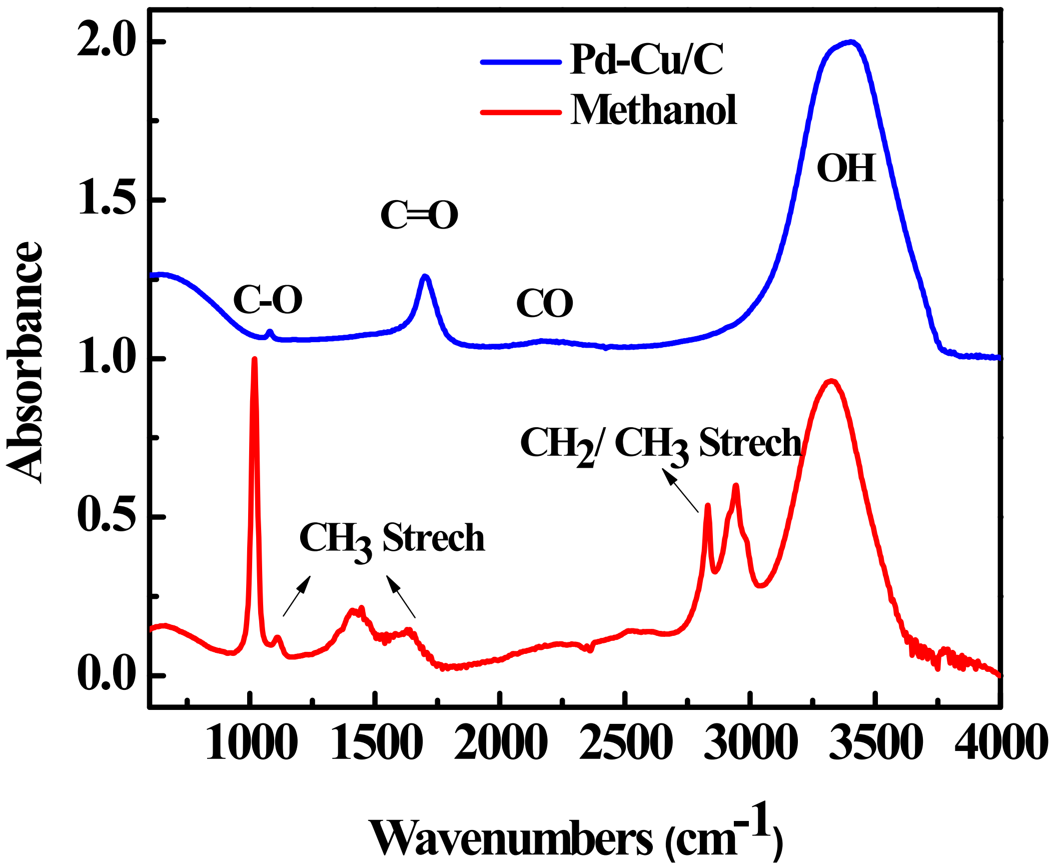

Figure S7. FTIR-Reflectance Spectra for Pd-Cu/C in 1M Methanol with 1M KOH solution

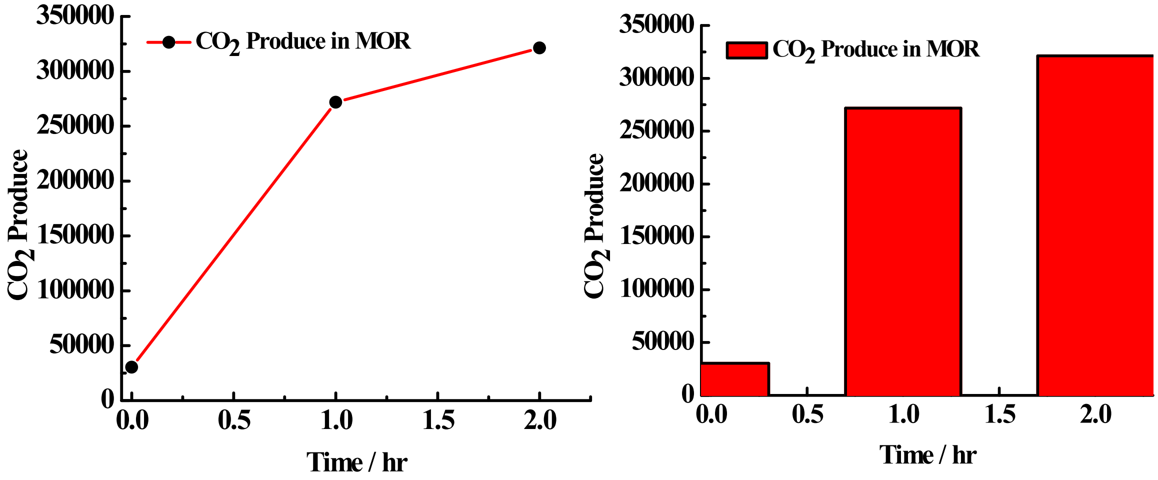

Figure S8. Pd-Cu/C in 1M Methanol with 1M KOH solution CO_2 production hourly by GC analysis.

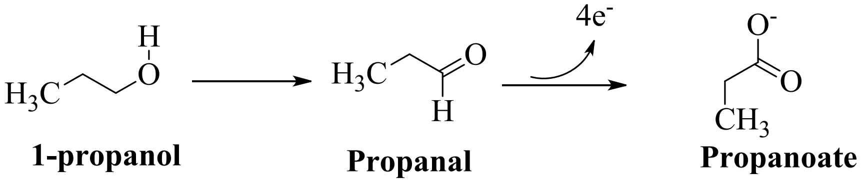

Scheme S1: Reaction pathway for 1-propanol oxidation mechanism.

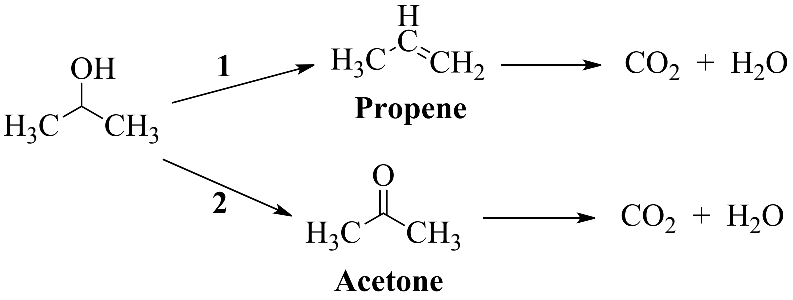

Scheme S2: Reaction pathway for 2-propanol oxidation mechanism.

$$\text{Pd-H}_{\text{abs/ads}} + \text{OH}^- \longrightarrow \text{Pd} + \text{H}_2\text{O} + e^- \tag{1}$$

$$\text{Pd} + \text{OH}^- \rightleftharpoons \text{Pd-OH}_{\text{ads}} + e^- \tag{2}$$

$$\text{Pd-OH}_{\text{ads}} + \text{OH}^- \rightleftharpoons \text{Pd-O} + \text{H}_2\text{O} + e^- \tag{3}$$

$$\text{Pd-OH}_{\text{ads}} + \text{Pd-OH}_{\text{ads}} \rightleftharpoons \text{Pd-O} + \text{H}_2\text{O} \tag{4}$$

$$\text{Cu} + 2\text{OH}^- \rightleftharpoons \text{Cu(OH)}_2 + 2e^- \tag{5}$$

$$\text{Pd-OH} + \text{Cu} \rightleftharpoons \text{CuOH} + \text{Pd} \tag{6}$$

$$\text{Pd-OH}_{\text{ads}} + \text{OH}^- \rightleftharpoons \text{Pd-O} + \text{H}_2\text{O} + e^- \tag{7}$$

$$\text{CH}_3\text{OH} + \text{H}_2\text{O} \longrightarrow \text{CO}_2 + 6\ \text{H}^+_{\text{aq}} + 6e^- \tag{8}$$

$$\text{Pd–CH}_2\text{OH} + 7\text{OH}^- \rightleftharpoons \text{Pd} + \text{CO}_3^{2-} + 5\text{H}_2\text{O} + 5e^- \tag{9}$$

$$\text{Pd–H} + \text{OH}^- \rightleftharpoons \text{Pd} + \text{H}_2\text{O} + e^- \tag{10}$$

$$\text{Pd} + \text{CH}_3\text{CH}_2\text{OH} \rightleftharpoons \text{Pd-(CH}_3\text{CH}_2\text{OH)}_{\text{ads}} \tag{11}$$

$$\text{Pd-(CH}_3\text{CH}_2\text{OH)}_{\text{ads}} + 3\text{OH}^- \longrightarrow \text{Pd-(CH}_3\text{CO)}_{\text{ads}} + 3\text{H}_2\text{O} + 3e^- \tag{12}$$

$$\text{Pd-(CH}_3\text{CO)}_{\text{ads}}\ \text{M-OH}_{\text{ads}} \longrightarrow \text{Pd-CH}_3\text{COOH} + \text{M} \quad (\text{M} = \text{Pd/Cu}) \tag{13}$$

$$\text{Pd-CH}_3\text{COOH} + \text{OH}^- \longrightarrow \text{Pd} + \text{CH}_3\text{COO}^- + \text{H}_2\text{O} \tag{14}$$

$$\text{PdCO} + \text{Cu(OH)}_2 \rightleftharpoons \text{Pd} + \text{Cu} + 2\text{H}^+ + \text{CO}_3^{2-} \tag{15}$$

$$\text{Pd-HCO} + \text{Cu(OH)}_2 \rightleftharpoons \text{Pd} + \text{CO}_3^{2-} + \text{Cu} + 3\text{H}^+ + e^- \tag{16}$$

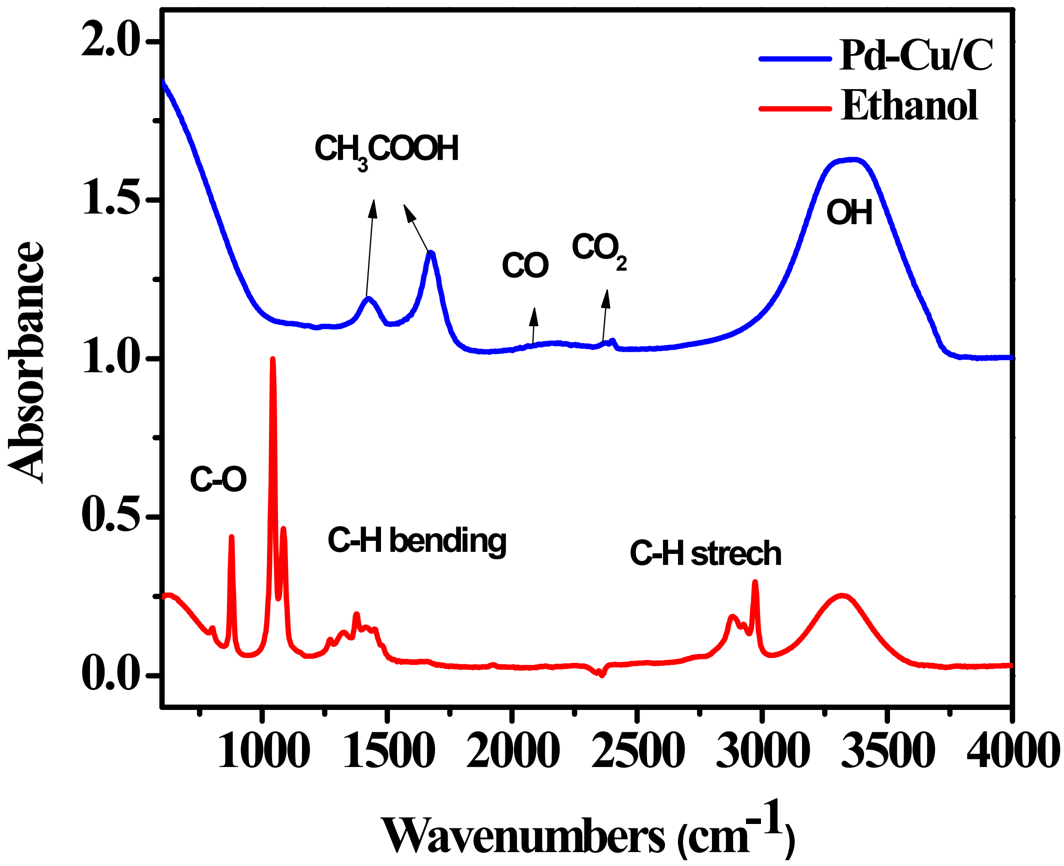

Figure S9. FTIR-Reflectance Spectra for Pd-Cu/C in 1M ethanol with 1M KOH solution.

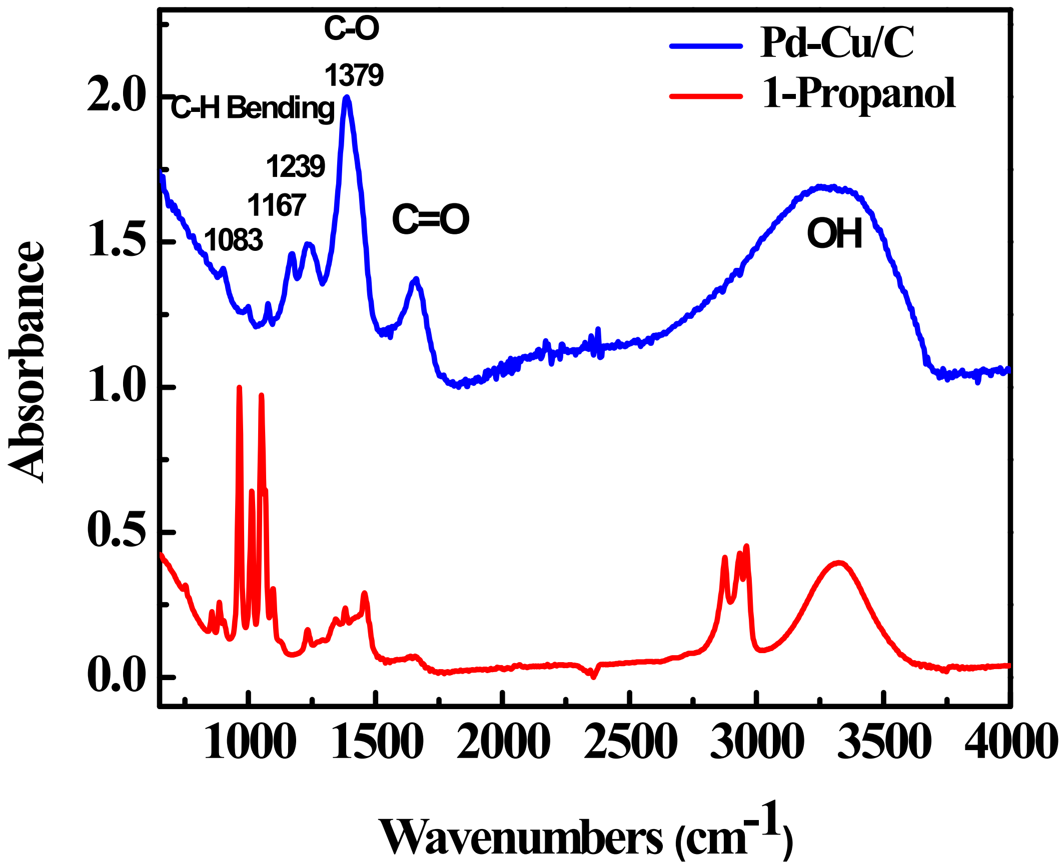

Figure S10. FTIR-Reflectance Spectra for Pd-Cu/C in 1M 1-propanol in 1M KOH solution.

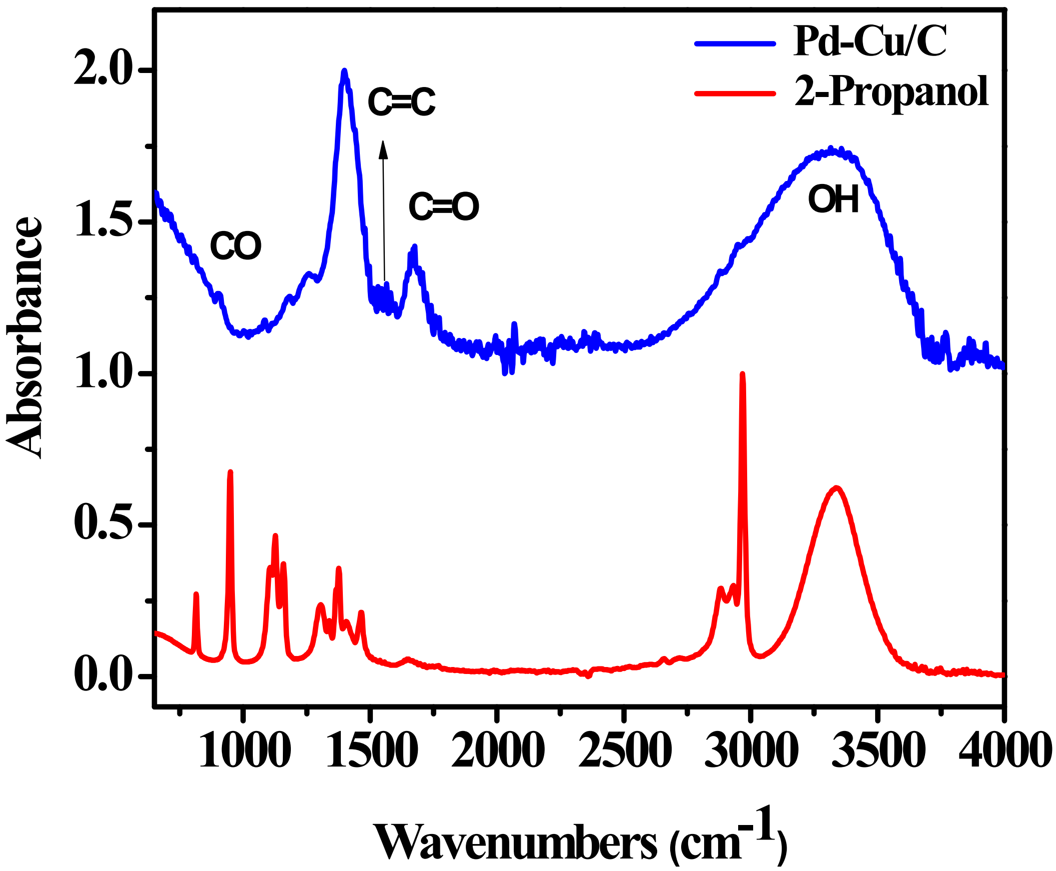

Figure S11. FTIR-Reflectance Spectra for Pd-Cu/C in 1M 2-propanol in 1M KOH solution.

References

1. K. Schlichte, T. Kratzke and S. Kaskel, *Microporous and Mesoporous Materials*, 2004, **73**, 81-88.
2. T. Takamura and K. i. Minamiyama, *Journal of The Electrochemical Society*, 1965, **112**, 333-335.
3. J. Prabhuram, R. Manoharan and H. Vasan, *Journal of applied electrochemistry*, 1998, **28**, 935-941.
4. M. Grdeń, J. Kotowski and A. Czerwiński, *Journal of Solid State Electrochemistry*, 2000, **4**, 273-278.
5. M. Breiter, *Journal of Electroanalytical Chemistry and Interfacial Electrochemistry*, 1977, **81**, 275-284.
6. V. Balaramachandran, K. Srinivasan and V. Kapali, *Corrosion science*, 1991, **32**, 185-191.
7. Z. Yin, Y. Zhang, K. Chen, J. Li, W. Li, P. Tang, H. Zhao, Q. Zhu, X. Bao and D. Ma, *Scientific reports*, 2014, **4**.
8. X. Xia, T. Iwasita, F. Ge and W. Vielstich, *Electrochimica Acta*, 1996, **41**, 711-718.
9. J. S. Spendelow and A. Wieckowski, *Physical Chemistry Chemical Physics*, 2007, **9**, 2654-2675.
10. J.-B. He, D.-Y. Lu and G.-P. Jin, *Applied Surface Science*, 2006, **253**, 689-697.
11. F. Gobal and R. Arab, *Journal of Electroanalytical Chemistry*, 2010, **647**, 66-73.
12. T. Cochell and A. Manthiram, *Langmuir*, 2012, **28**, 1579-1587.
13. Z.-Y. Shih, C.-W. Wang, G. Xu and H.-T. Chang, *Journal of Materials Chemistry A*, 2013, **1**, 4773-4778.